

Multiscale Modeling of Reconstructed Tricalcium Silicate using NASA Multiscale Analysis Tool

Vishnu Saseendran¹, and Namiko Yamamoto²

Department of Aerospace Engineering, The Pennsylvania State University, University Park, PA, 16802 United States

Ibrahim Kaleel³, Evan J. Pineda⁴, and Brett A. Bednarcyk⁵

NASA Glenn Research Center, Cleveland, OH, 44135 United States

Peter Collins⁶, and Aleksandra Radlińska⁷

Department of Civil and Environmental Engineering, The Pennsylvania State University, University Park, PA, 16802 United States

To study microstructure characteristics of cementitious materials hydrated in space; previously, cement binder formations were processed under microgravity conditions and was further compared against ground-based experiments. For accurate estimation of process-structure-property linkage, particularly on samples hydrated in the microgravity environment, it is desired to have a high-fidelity volumetric representation of the microstructure. However, owing to small sample size and high porosity of the space-returned samples, conventional experimental characterization techniques are not viable. Hence, a deep learning-based reconstruction algorithm was employed to obtain high fidelity 3D volumes from sparse high resolution 2D Scanning Electron Microscopy (SEM) images, as inputs to micromechanics-based modeling. This machine learning-based reconstruction methodology validated against low-order statistical descriptors, captured the microstructural topology of both sample types (ground, 1g and microgravity, μg). Due to the lack of gravity, hydration products of the samples processed in space differed from those processed-on ground. Such AI-generated virtual samples were analyzed in a multiscale recursive micromechanics approach using the NASA Multiscale Analysis Tool (NASMAT). Here, we present a methodology to rapidly integrate and evaluate these AI-generated volumes in NASMAT. The synthesized microstructural volumes are directly employed as Representative Volume Elements (RVEs) to preserve the fidelity (1 pixel = 0.54 μm). Invariably, analysis of such largescale problems (512^3 voxels) requires huge amount of computational resources. By taking advantage of the NASMAT architecture, we also focused on systematic multiscale integration of these AI-reconstructed virtual volumes to reduce the computational demands. In this work, this methodology is demonstrated on the ground-based, 1g samples. The estimated stiffness value of 15.90 GPa is comparable to experimentally obtained modulus of hydrated tricalcium silicate sample. The workflow presented here paves the way for utilizing the NASMAT tool to

¹ Assistant Research Professor, Department of Aerospace Engineering, The Pennsylvania State University, AIAA Member

² Associate Professor, Department of Aerospace Engineering, The Pennsylvania State University. AIAA Senior Member.

³ Postdoctoral Fellow, NASA Postdoc Program, AIAA Member.

⁴ Research Aerospace Engineer, NASA Glenn Multiscale and Multiphysics Modeling Branch, AIAA Associate Fellow.

⁵ Research Aerospace Engineer, NASA Glenn Multiscale and Multiphysics Modeling Branch, AIAA Associate Fellow.

⁶ Ph.D. Candidate, Department of Civil and Environmental Engineering, The Pennsylvania State University.

⁷ Associate Professor, Department of Civil and Environmental Engineering, The Pennsylvania State University.

perform multiscale analyses of other multi-phase material systems using either 3D virtual datasets synthesized using AI or obtained via micro-CT.

I. Introduction

To protect both crew and equipment during long-duration space exploration missions, habitats are necessary on extraterrestrial bodies such as the Moon and Mars. In addition, landing pads are required for the spacecrafts to reliably land and launch from these bodies. Given the prohibitive cost of transporting materials into space, it is envisioned that *in situ* materials such as the lunar regolith will be employed for constructing habitats and launch pads with the aid of cement-like binders. The solidification of these cement binders under the influence of reduced microgravity ($10^{-6} g$ or μg) was previously studied under the ambit of the project titled – “Microgravity Investigation of Cement Solidification (MICS)” [1, 2]. To focus on the influence of reduced gravity and how it affects the microstructural formation of cement-binder formation, pure compounds - tricalcium silicate (Ca_3SiO_5 : C_3S in cement notation) and tricalcium aluminate ($Ca_3Al_2O_6$: C_3A in cement notation) were analyzed under both terrestrial (1g) as well as μg conditions. Note, C_3S constitutes $\sim 50 - 70$ % of Ordinary Portland Cement (OPC) by mass [3], and is an important component that governs the hydration of OPC. Hence, the C_3S microstructure directly influences the physical and mechanical properties of the hardened cement paste. Due to the size limitation and highly porous nature (~ 70 %) of the space returned C_3S samples [2], traditional experimental characterization techniques such as flexure or compression testing are not viable. Therefore, numerical modeling is currently the only way to evaluate mechanical properties to perform structure-property predictions of these samples. To reliably predict mechanical and transport properties of these cement binders using a numerical code, 3D representations which capture the unique microstructure morphology are required. The hydration products in the μg samples, namely, calcium silicate hydrate (C-S-H), portlandite (CH), and porosity exhibited distinct and unique characteristics compared to the 1g samples; C-S-H and CH – cement chemistry notation, C = CaO, S = SiO_2 , and H = H_2O followed throughout this manuscript.

Previously, a deep learning-based microstructure reconstruction approach [4] was employed to synthesize 3D microstructures of both μg and 1g samples (see **Figure 1**) from high-resolution of Scanning Electron Microscopy (SEM) images. These reconstructed volumes successfully captured randomly oriented elongated plate-like morphology of the CH phase distinct to the space returned samples. For instance, a larger prismatic morphology of CH crystallite formation due to the absence of gravity was captured in the μg reconstructed volume. Individual phases were discerned from both SEM images (utilized as exemplars) as well as the 3D virtual data by greyscale-based thresholding, following overflow method coupled with local-minima approach [4]. In addition, statistical descriptors, two-point correlation function, $S_2(r)$, two-point cluster function, $C_2(r)$, and linear-path function, $L_2(r)$ [5] were employed to validate the randomness and distribution of various phases contained in both μg and 1g samples [6]. Both qualitative and quantitative assessments of these synthesized samples indicated that such AI-based 3D reconstructions are stable in comparison to micro-CT virtual data [6]. These reconstructed volumes are then directly employed as Repeating Unit Cells (RUCs) in the advanced micromechanical-based numerical code – NASA Multiscale Analysis Tool (NASMAT) for mechanical characterization. Specifically, the micromechanics model High-Fidelity Generalized Method of Cells (HFGMC) in the NASMAT code was employed to obtain both Young’s modulus and Poisson’s ratio of the reconstructed microstructure volumes. In this work, we discuss numerical results of only 1g samples.

The deep learning-based reconstruction methodology [4] enables utilization of high-resolution exemplars to synthesize ensembles of virtual volumes. Thus, by employing such high-resolution (1 pixel = $0.54 \mu m$) exemplars for reconstruction, the generated 3D virtual datasets were able to achieve better representation of each phase. Such a high-quality representation of microstructure morphology augments the fidelity of the analysis. However, to conduct a probabilistic analysis, several ensembles of such 3D microstructure reconstructions need to be solved in NASMAT. For instance, for the virtual dataset of 256^3 voxels shown in **Figure 1**, NASMAT needs to homogenize as many stiffness tensor terms which invariably requires a prohibitive amount of memory. On the other hand, a separate sensitivity study [6] for AI-based 3D reconstruction concluded that for the given pixel resolution of $0.54 \mu m$, at least 512×512 pixels ($276.5 \times 276.5 \mu m^2$) exemplar size is required for the μg samples. This is based on common design guidelines, wherein the recommended RUC size for mechanical characterization is at least $5 - 10x$ that of the characteristic size of the phase. Here, in the case of μg samples, portlandite phase with its distinct elongated plate-like morphology governs the characteristic length-scale ($100 - 125 \mu m$) [6]. To enable analysis of such large-scale problems, we present a strategy in this work, wherein the generated volumes are split into an arbitrary number of

multiscale analysis incorporating smaller RUCs at the lower sub volumes. Homogenization is performed at all scales in order to obtain the bulk properties of the sample. By exploiting the recursive nature of the NASMAT tool, we first perform multiscale analysis of 1g samples to obtain mechanical properties (Young’s modulus and Poisson’s ratio). Since the properties of interest are considered linear at this time, the absences of true separation of scales in the multiscale analysis does not introduce significant error into the model. However, the same multiscale strategy may not be feasible if the constituent behavior is nonlinear. The workflow presented here will be extended to analyze μg samples as well as to pave the way for multiscale analysis of conventional large-scale virtual data, including micro-CT volumes to be efficiently solved using NASMAT.


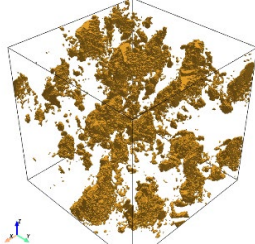
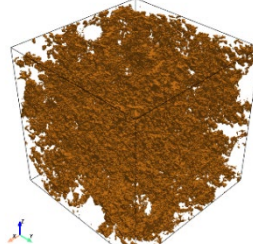
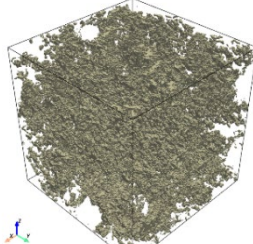
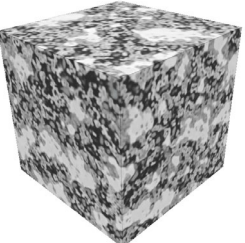
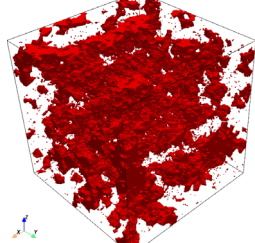
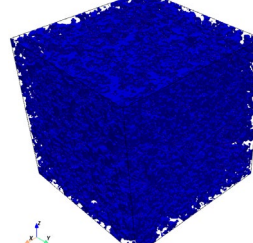
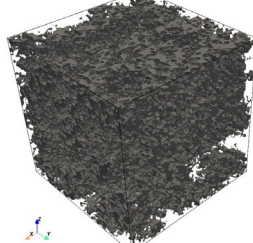
Reconstructed Volumes	CH	C-S-H	Porosity
 <p>μg sample</p>	 <p>11.7%</p>	 <p>20.4%</p>	 <p>68.47%</p>
 <p>1g sample</p>	 <p>17.4%</p>	 <p>33.9%</p>	 <p>49.3%</p>

Fig 1. Reconstructed 3D volumes (256^3 voxels) of both 1g and μg samples and respective phases segmented using greyscale-based thresholding utilizing an overflow method coupled with local minima approach [4]. An exemplar size 256×256 pixels (with $0.54 \mu\text{m}$ resolution) is shown here. Individual % phase composition is provided beneath each phase.

II. Methodology

Study of pure compounds, such as C_3S , a prime constituent in OPC aids in understanding the nature of microstructural formation and will lead to comparison of ground and space-cured samples. In addition, from the perspective of mechanical characterization, a thorough characterization of such pure phases invariably renders the analysis workflow robust. The success of any multiscale micromechanics-based analysis of a multi-phase material system depends on the accurate description of the size and morphology of individual phases in a RUC. In this work, the morphology of individual phases is represented using 3D RUCs, obtained via a deep learning-based 2D to 3D reconstruction framework initially proposed by Gutierrez et al. [7], and extended to cementitious system in our previous work [4]. This synthesized virtual data was segmented using a histogram-based greyscale thresholding approach and the resulting RUCs are directly inputted to NASMAT code (see **Figure 2**). In this section, we briefly provide an overview of this AI-based reconstruction methodology [4, 6] and NASMAT code [8], followed by multiscale integration of the synthesized volumes into the NASMAT framework. A schematic illustration of the workflow is presented in **Figure 2**. Owing to the sheer size of this synthesized volume (512^3 voxels; $0.54 \mu\text{m}$ resolution), a stand-alone algorithm is developed here that allows for any arbitrary number of sub volumes to be generated from a given volume (AI-reconstructed or traditional micro-CT -based). This in-turn reduces the required computational demand, and here, this multiscale approach applied to C_3S is modeled using the High-Fidelity

Generalized Method of Cells (HFGMC) [9]. Note, that the NASMAT tool, by its recursive nature allows to define any arbitrary number of sub volumes. This enables the analysis of such large-scale problems containing high-resolution 3D virtual data with modest memory and compute time requirements.

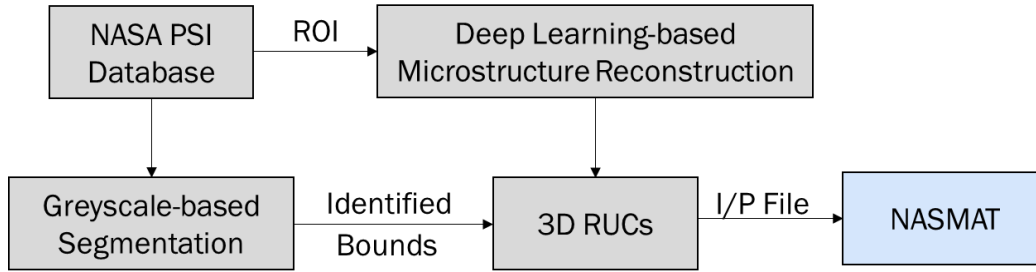


Fig 2. Workflow: Triply periodic user-defined RUC definition of reconstructed C_3S microstructure virtual volumes with chosen exemplar(s) taken from the NASA PSI database. Multiscale analysis in NASMAT is achieved via an in-house developed Python-based script that enables automatic generation of input files by portioning a virtual volume into a pre-defined arbitrary length-scales.

A. Brief Overview of NASMAT

NASMAT's design and architecture prioritize key aspects such as modularity, upgradability, maintainability, interoperability, utility, and scalability [8]. The NASMAT procedures and data types exhibit a recursive nature, facilitating the creation of the Multiscale Recursive Micromechanics (MsRM) framework [10]. The code by its inherent modular design employs several recursive procedures and subroutines. Hence, this code can also be easily adapted by interchanging the modules allowing for flexible formulation to address a particular multiscale problem. For instance, NASMAT has been successfully employed to perform multiscale failure simulations of 3D woven composites [11], unidirectional fiber-reinforced composites [12], braided composites [13], and have also been successfully integrated with Molecular Dynamics (MD) at its lowest tier to study thermoplastics [14] and nanoplatelets [15]. Here we utilize multiscale modeling to ascertain the mechanical properties of the reconstructed C_3S virtual volumes, and exploit the recursive nature of NASMAT to analyze these AI-synthesized samples.

Note, that NASMAT facilitates “plug and play” functionality and hence, is capable of invoking various micromechanics theories such as the Generalized Method of Cells (GMC), the Parametric HFGMC, Carerra Unified Formulation (CUF), and the Mori-Tanaka Mean Field Theory (MT) [16-19]. The semi-analytical method, the High-Fidelity Generalized Method of Cells (HFGMC) [9] was selected here to predict the mechanical properties of the hydrated C_3S samples. Here, the effective mechanical properties of the reconstructed C_3S is computed via homogenization using the HFGMC model, and the overall utility of the chosen micromechanics model is also verified.

B. Deep Learning-based Microstructure Reconstruction & Phase Allocation in User-defined RUCs

The tricalcium silicate samples, C_3S , evaluated in this work was cured with lime water at a water-to-cement ratio (w/c) of 2.0 by mass. This high w/c ratio enhanced crystal growth by coarsening the porosity. Moreover, magnifying the effect of overall microstructural development aids in understanding the μg effects. The fabrication details of these samples can be found elsewhere [1]. The fractured surfaces of the hydrated samples were dried under a vacuum, mounted in acrylic resin, and polished. The Backscattered Electron (BSE) images of the polished sections were taken with a magnification of 500x and was used as exemplars in the 2D – 3D reconstruction framework, refer to [4,6] and see **Figure 1**.

Image reconstruction has been ubiquitously applied in the field of computer vision and graphics. In the materials science community, Markov Random Field (MRF) based microstructure reconstruction technique is prominent [20]. With the recent advancement in Convolutional Neural Networks (CNNs) in the field of computer vision, machine learning-based approaches, especially transfer-learning based microstructure reconstruction techniques are widely becoming popular [21-23]. Amongst such machine learning-based techniques, a computationally efficient approach based on texture-synthesis [7] was employed by the authors previously [4] to synthesize ensembles of 3D microstructures of both μg and 1g samples. In this framework, initially proposed by Gutierrez et al. [7], a compact

generative framework based on CNN was employed. A pre-trained deep network architecture, namely, VGG-19 [24] is utilized, and a volumetric perceptual loss function is defined that optimizes the statistical features of the generated volume to that of the input 2D exemplar. By comparing only 2D slices of the synthesized volume across a set of desired directions with the exemplar, this methodology enables computationally efficient microstructure reconstruction. Note, the pre-trained deep CNN model, VGG-19 used in this model is trained on ImageNet dataset [25] and accepts a 2D image with a 3-channel (RGB) as input. The 2D greyscale exemplars (512 x 512 pixels) selected from the BSE images stored in the NASA PSI database was converted to a 3-channel representation using the OpenCV library. During training, statistical features of the exemplar is compared to the slices extracted from the synthesized volume using feature maps. The reconstructed C₃S microstructural volume is then directly incorporated as a user-defined 3D RUC in NASMAT, refer to **Figures 1** and **2**. Compared to our previous work in [4], we augmented the reconstruction here by adding more target images in the reconstruction algorithm. By carefully selecting exemplars containing various CH crystals, the resulting synthesized volume captured the distinct plate-like morphology of CH crystals in μg samples very well (**Figure 2**). The increase in computational time for training was not that significant.

Invariably to define the material card of this user-defined 3D RUC, each phase in the reconstructed C₃S microstructural volume needs to be identified. Previously, the SEM images of both μg and 1g samples, stored in the NASA PSI database was analyzed using a greyscale-based thresholding approach [4] to discern various hydration products (CH, C-S-H and porosity). Firstly, the images were treated using a Sigma filter (with $\sigma = 2.0$) [26] and then analyzed using an in-house script that identifies various bounds in the histogram to distinct to each phase. A local-minima based approach was used to identify the bound in the histogram between CH and C-S-H phases. To circumvent edge effects attributed to the high mismatch of atomic numbers between porosity and the C-S-H phase, overflow method [27] was used to identify the porosity/C-S-H boundary. The image analysis was benchmarked against the total porosity for both μg and 1g samples using the Mercury Intrusion Porosimetry (MIP) technique [1]. For a detailed overview of the greyscale-based image segmentation workflow used to identify each phase in hydrated C₃S samples, refer to our previous work [4]. A short Python-based script was developed to assign individual phase on each voxel of the reconstructed C₃S volume based on its intensity (see **Figure 2**). For material assignment, depending on each voxel intensity, following NASMAT material notation, M = 1; CH, M = 2; C-S-H, and M = 3; Porosity were assigned to each of the 512³ voxels. A detailed discussion on the hierarchical multiscale modeling strategy devised to study C₃S virtual data is provided in the subsequent section.

C. Multiscale Integration of Reconstructed C₃S Volumes

The phase-assigned reconstructed 3D virtual data is directly inputted into the NASMAT tool as a user-defined RUC to assess effective stiffness properties. However, due to the prohibitive amount of memory required, simulation of the reconstructed virtual volume as a single RUC (512³ subcells) is very challenging. Hence, multiscale modeling of C₃S microstructure spanning multiple concurrent length scales was carried out to obtain the mechanical properties. The schematic illustration of such a multiscale modeling setting in which the reconstructed volume is partitioned into arbitrary length-scale is presented in **Figure 3**. Within the MsRM approach, any arbitrary number of scales can be included. The MsRM framework of NASMAT allows information to be passed down the scales through localization, and up the scales through homogenization [12]. Here, Level 0 represents the highest RUC (512³ voxels; resolution 0.54 $\mu\text{m}/\text{pixel}$). The effective properties of each subcell are obtained via the homogenization of the RUCs at the subsequent scales defined below. The scales are linked by equilibrating the homogenized average stress, strain and stiffness tensors at a particular level, i to the local stress, strain, and stiffness tensors of a given subcell at level, $i - 1$ [8, 10]. It should be noted that in these analyses there is no separation in scale as is typically required for multiscale analysis. However, the error introduced is minimal since the properties of interest obtained through homogenization are linear.

A stand-alone algorithm was developed that allows for partitioning of a given virtual volume (AI-generated or micro-CT) into multiple sub volumes (see **Table 1**). For a given heterogenous material, the algorithm (see pseudocode presented in **Table 1**) automatically assembles a NASMAT input file by splitting the given RUC to any user-defined consequent sub volumes. The metadata regarding NASMAT header files are automatically handled by the algorithm requiring no further modification to the script prior to submission. The schema presented in **Figure 1** shows two cases, wherein the reconstructed C₃S 1g sample is partitioned into two multiple sub volumes. Note, that while assembling the code for submission in NASMAT, material properties must be defined and each voxel in the virtual volume must be assigned a distinct material. Here, CH, C-S-H and porosity phases are assigned to each voxel based on the greyscale bounds identified using a combined overflow method and local minima-based approach [4]. This material assignment

is performed at its lowest sub volume; for instance, at Level-2 comprising of 4^3 voxels (see **Figure 3**), the algorithm compares the greyscale intensity with the defined bounds and allocates a material. By exploiting the recursive framework in NASMAT, the homogenized properties are then assigned to next upper level (Level 1 in this case). In addition, the presented schema allows to perform failure analysis of microstructures with increased fidelity. For instance, advanced 2D to 3D reconstruction tools [4, 6, 20 - 23], enables generation of virtual data with higher pixel resolution. Hence, the current approach enables investigation of such high-resolution 3D microstructural volumes in NASMAT. Moreover, on occasions where there is limited availability of computer nodes at runtime or limited memory, the current approach aids to break down the analysis domain into further smaller volumes at an arbitrary number of sub volumes, thus reducing the computational demands. The ability to partition a given RUC to a pre-defined number of scales also allows the user to quickly evaluate the utility of various micromechanical models.

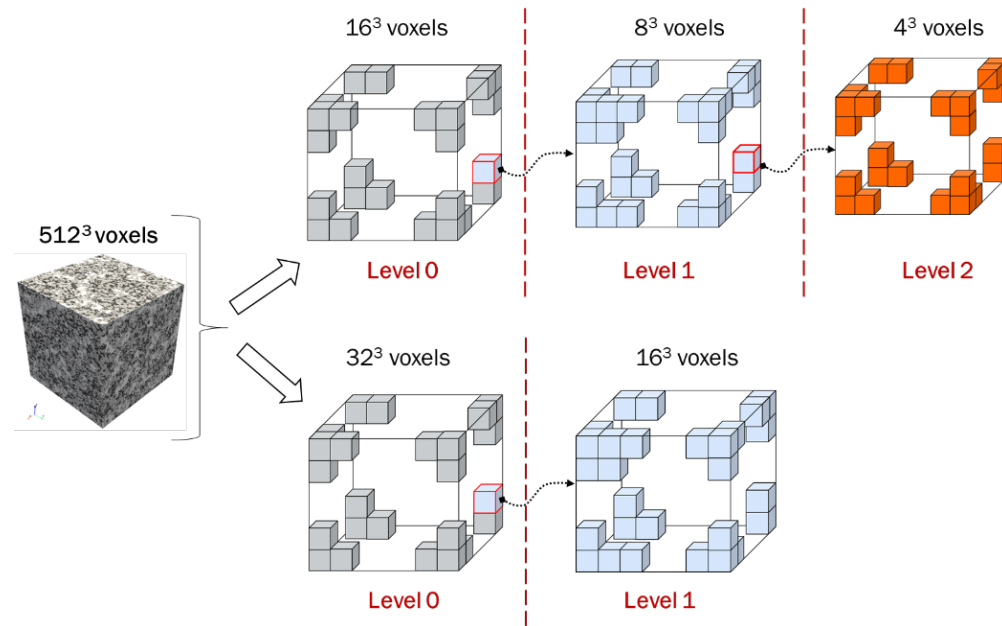


Fig 3. Schematic illustration of the proposed multiscale analysis framework in which the AI-assisted reconstructed C_3S virtual volume (1g sample) is partitioned into user-defined arbitrary sub volumes; top: 512^3 volume partitioned into 16^3 voxels in Level 0, 8^3 voxels in Level 1 and 4^3 voxels in Level 2 and bottom 512^3 volume partitioned into 32^3 voxels in Level 0 and 16^3 voxels in Level 1. During homogenization, the effective stiffness matrix for the 3D RUC is passed up from the bottom-most scale to Level 0.

Table 1. Pseudocode for generating multiscale NASMAT input file by partitioning a given RUC volume (reconstructed or micro-CT) of a heterogenous material into hierarchical sub volumes.

Algorithm 1 Pseudocode to split any virtual volume to arbitrary number of sub volumes and create NASMAT input file.

Require: $n_{Level} \geq 1$ ▷ Must be greater than 1

Inputs:

n_{Level}
Grayscale bounds
Reconstructed Volume ▷ AI-reconstructed or micro-CT

Initialize:

RUC as a 3D array
NASMAT Input file header
 $N_{subRUC,n}$
 $MSM^n = 0$

while $n_{Level} \neq 1$ **do**

Extract sub-RUCs ($N_{subRUC,n}$) from the input volume
Update metadata: NASMAT header
Update counters: $MSM^n = -17 - N_{subRUC,n}^3$

for n_{Level} is largest **do**

RUC: Assign a material ID based on grayscale values
 $MSM^n = -17 - MSM^n$:Update counters

end for

end while

III. Results and Discussion

The phase-assigned reconstructed 3D virtual data of 1g C₃S sample are directly inputted into the NASMAT code as a triply-periodic, user-defined, multiscale RUC to assess the effective stiffness properties. Here, the numerical results for the case wherein, the RUC is partitioned into 16³ in Level 1 and 32³ voxels in Level 0 is presented. A standard linear elastic model was considered for each phase. The material properties of individual phases (C-S-H and CH) were taken from the literature, where the reported values are obtained using a nanoindentation study [28]. The E-modulus and Poisson’s ratio of the C-S-H phase were 21.7 GPa and 0.25, respectively. For the CH crystals, E-modulus 35 GPa and Poisson’s ratio 0.31 was assumed. Due to the high w/c ratio used in this study, hydrated C₃S samples under 1g condition exhibited porosity of 48.4% [1, 4, 6]. In such highly porous samples (see **Figure 1**), the failure mechanism is driven by the porosity. Here, the modulus of the porosity was chosen as 1 MPa. As previously mentioned, the stiffness properties of the monophasic materials (C-S-H and CH) have been taken from the nanoindentation study in the literature. These methods postulate that there exist two types of C-S-H and validity of utilizing such nanoindentation and deconvolution techniques is highly debated. It must also be noted that the modulus considered here for both C-S-H and CH phases assume non-porous monophasic composition. However, for initial comparison, the stiffness values obtained from the nanoindentation study can be used. The analysis was run on a single CPU; results are presented in **Table 1**, along with the memory used and wall time. The total recorded analysis time for the case wherein, the reconstructed 512³ voxels is partitioned into two levels is 23.02h with a total memory usage of 55.41 GB.

Table 2. Summary of multiscale analysis on reconstructed 1g C₃S samples portioned into sub volumes having Level 0: 32³ voxels and Level 1: 16³ voxels.

Mechanical Properties		
E_{11}	E_{22}	E_{33}
15.90	9.02	15.83
G_{12}	G_{23}	G_{13}
3.83	3.06	5.57
ν_{12}	ν_{23}	ν_{13}
0.25	0.12	0.23
Resource Usage		

CPU Time Used	23.02 h
Memory Used	55.41 GB

The numerical results obtained here (**Table 1**) are compared against a 32-year-old hydrated C₃S sample with a reported E-modulus = 18.84 GPa at 43.35% porosity [29]. The numerically obtained results (E_{11}) are comparable to stiffness value presented in [29], obtained via microindentation testing. Microindentation of a multiphase composite such as C₃S enables robust measurement of stiffness properties, as the interaction volume beneath the indenter that arises in nanoindentation test and surface roughness influences are circumvented. Additionally, the microindentation data provides a composite response and the contribution of individual phases in hydrated C₃S cannot be separated from the results. In the hydrated C₃S, C-S-H phase is the principle binding phase and CH are present as stiff inclusions that prevent deformation.

Initial numerical results presented in this work exploiting the recursive nature of NASMAT to devise multiscale integration of reconstructed C₃S volumes looks promising. The discrepancy in E_{22} value compared to E_{11} and E_{33} (by almost ~ 50%) is not well understood. It may be attributed to the reconstructed volume itself, which in turn is governed by the chosen exemplar. In general, hydrated cement is considered to be isotropic in nature. Moreover, mechanical properties such as Young’s modulus and hardness are dependent on humidity. In the 1g sample, despite having high porosity content (attributed to high w/c ratio = 2.0), the CH crystals are uniformly distributed (see **Figure 1**). For the reconstructed 1g sample volumes, the CH phase composition varied between 8 – 17.40 %, porosity varied 49 – 52 %, and the C-S-H matrix composition was estimated to be 34 – 40 % [4, 6]. Additionally, the spatial distribution of both CH crystal and porosity phases were both qualitatively and quantitatively affirmed with the aid of micro-CT data [6]. For quantitative evaluation, low-order statistical functions, two-point correlation function, $S_2(r)$, two-point cluster function, $C_2(r)$, and linear-path function, $L_2(r)$ were used [6]. Future efforts will involve probabilistic estimation of stiffness properties following the multiscale integration strategy presented in this work.

IV. Conclusion

For highly porous samples, in particular, cementitious materials hydrated in space conventional mechanical characterization is not viable. Therefore, to estimate mechanical properties numerical assessment can be carried out with the aid of 3D virtual data generated from their high-resolution 2D SEM images. This work provides a framework to carry out analysis of such high-resolution reconstructed virtual data. To reduce the demand of computational resources, a multiscale analysis in NASMAT wherein, the highly porous synthesized volume is partitioned into multiple sub volumes is introduced. This multiscale representation of the reconstructed volume led to effective computation of stiffness properties in NASMAT. Numerical results pertaining to reconstructed C₃S samples hydrated on ground is presented. The numerically predicted stiffness value of 15.90 GPa is comparable to experimentally values in the literature. Note, that the results presented here are comparable to hydrated C₃S samples exhibiting similar porosity. Furthermore, since our previously reported work, the reconstructed samples, especially that of μg samples have been improved. These improvements were caused by adding more exemplars as input images in the reconstruction methodology. By adding more target images along the desired orthogonal directions, the distinct plate-like features of CH morphology were captured very well. The study also aims to present the user with an automated methodology to effectively partition a given virtual volume data into pre-defined length scales, and assemble a NASMAT input script by assigning each voxel with a distinct phase following greyscale-based phase segmentation. In future, the workflow presented here will be extended to analyze μg samples as well as paves the way for traditional large-scale virtual data, e.g., micro-CT to be efficiently solved using NASMAT.

Acknowledgments

This research is funded by NASA’s Physical Sciences Research Program (80NSSC22K0083). The NASA authors acknowledge support from the NASA Aeronautics Transformational Tools and Technologies Project.

References

- [1] Moraes Neves, J., Collins, P. J., Wilkerson, R. P., Grugel, R. N., and Radlińska, A.,” Microgravity effect on microstructural development of tri-calcium silicate (C3S) paste,” *Frontiers in Materials*, Vol. 83, No. 6, 2019, pp. 1-12. doi: 10.3389/fmats.2019.00083

- [2] Collins, P. J., Grugel, R. N., and Radlińska, A., "Hydration of tricalcium aluminate and gypsum pastes on the International Space Station," *Construction and Building Materials*, vol. 285, published online 24 May. 2021. doi: <https://doi.org/10.1016/j.conbuildmat.2021.122919>
- [3] Gartner, E. M., J. F. Young, D. A. Damidot, and I. Jawed. "Hydration of Portland cement." *Structure and performance of cements 2* (2002): 57-113.
- [4] Saseendran, Vishnu, Namiko Yamamoto, Peter Collins, Aleksandra Radlinska, Evan J. Pineda, and Brett A. Bednarczyk. "Reconstruction of Tricalcium Silicate Microstructures for Repeating Unit Cell Analysis." In *AIAA Scitech 2023 Forum*, p. 2025. 2023.
- [5] Torquato, Salvatore, and H. W. Haslach Jr. "Random heterogeneous materials: microstructure and macroscopic properties." *Appl. Mech. Rev.* 55, no. 4 (2002): B62-B63.
- [6] Saseendran, Vishnu, Namiko Yamamoto, Peter Collins, Aleksandra Radlinska, Sara Mueller, and Enrique M. Jackson. "Unlocking the Potential: Analyzing 3D Microstructure of Small-scale Cement Samples from Space using Deep Learning." *npj Microgravity*. 2023.
- [7] Gutierrez, Jorge, Julien Rabin, Bruno Galerne, and Thomas Hurtut. "On demand solid texture synthesis using deep 3d networks." In *Computer Graphics Forum*, vol. 39, no. 1, pp. 511-530. 2020.
- [8] Pineda, Evan J., Brett A. Bednarczyk, Trenton M. Ricks, Steven M. Arnold, and Grant Henson. "Efficient multiscale recursive micromechanics of composites for engineering applications." *International Journal for Multiscale Computational Engineering* 19, no. 4 (2021).
- [9] Aboudi, J., Pindera, M. J., & Arnold, S. M. (2001). Linear thermoelastic higher-order theory for periodic multiphase materials. *J. Appl. Mech.*, 68(5), 697-707.
- [10] Pineda, Evan J., Trenton M. Ricks, Brett A. Bednarczyk, and Steven M. Arnold. "Benchmarking and performance of the NASA Multiscale Analysis Tool." In *AIAA Scitech 2021 Forum*, p. 1351. 2021.
- [11] Pineda, Evan J., Brett A. Bednarczyk, Trenton M. Ricks, Babak Farrokh, and Wade Jackson. "Multiscale failure analysis of a 3D woven composite containing manufacturing induced voids and disbonds." *Composites Part A: Applied Science and Manufacturing* 156 (2022): 106844.
- [12] Pineda, Evan J., Brett A. Bednarczyk, Anthony M. Waas, and Steven M. Arnold. "Progressive failure of a unidirectional fiber-reinforced composite using the method of cells: Discretization objective computational results." *International Journal of Solids and Structures* 50, no. 9 (2013): 1203-1216.
- [13] Liu, Kuang C., Aditi Chattopadhyay, Brett Bednarczyk, and Steven M. Arnold. "Efficient multiscale modeling framework for triaxially braided composites using generalized method of cells." *Journal of Aerospace Engineering* 24, no. 2 (2011): 162-169.
- [14] Pisani, William A., Matthew S. Radue, Sorayot Chinkanjanarot, Brett A. Bednarczyk, Evan J. Pineda, Kevin Waters, Ravindra Pandey, Julia A. King, and Gregory M. Odegard. "Multiscale modeling of PEEK using reactive molecular dynamics modeling and micromechanics." *Polymer* 163 (2019): 96-105.
- [15] Hadden, Cameron M., Danielle René Klimek-McDonald, Evan J. Pineda, Julie A. King, Alex M. Reichanadter, Ibrahim Miskioglu, S. Gowtham, and Gregory M. Odegard. "Mechanical properties of graphene nanoplatelet/carbon fiber/epoxy hybrid composites: Multiscale modeling and experiments." *Carbon* 95 (2015): 100-112.
- [16] Aboudi, Jacob, Steven M. Arnold, and Brett A. Bednarczyk. *Micromechanics of composite materials: a generalized multiscale analysis approach*. Butterworth-Heinemann, 2013.
- [17] Haj-Ali, Rami, and Jacob Aboudi. "A new and general formulation of the parametric HFGMC micromechanical method for two and three-dimensional multi-phase composites." *International Journal of Solids and Structures* 50, no. 6 (2013): 907-919.
- [18] Carrera, Erasmo, Maria Maiaru, Marco Petrolo, and Gaetano Giunta. "A refined 1D element for the structural analysis of single and multiple fiber/matrix cells." *Composite Structures* 96 (2013): 455-468.
- [19] Mori, Tanaka, and Kohichi Tanaka. "Average stress in matrix and average elastic energy of materials with misfitting inclusions." *Acta metallurgica* 21, no. 5 (1973): 571-574.
- [20] Sundararaghavan, Veera. "Reconstruction of three-dimensional anisotropic microstructures from two-dimensional micrographs imaged on orthogonal planes." *Integrating Materials and Manufacturing Innovation* 3, no. 1 (2014): 240-250.
- [21] Lubbers, Nicholas, Turab Lookman, and Kipton Barros. "Inferring low-dimensional microstructure representations using convolutional neural networks." *Physical Review E* 96, no. 5 (2017): 052111.
- [22] Bostanabad, Ramin. "Reconstruction of 3D microstructures from 2D images via transfer learning." *Computer-Aided Design* 128 (2020): 102906.

- [23] Li, Xiaolin, Yichi Zhang, He Zhao, Craig Burkhart, L. Catherine Brinson, and Wei Chen. "A transfer learning approach for microstructure reconstruction and structure-property predictions." *Scientific reports* 8, no. 1 (2018): 13461.
- [24] Simonyan, Karen, and Andrew Zisserman. "Very deep convolutional networks for large-scale image recognition." *arXiv preprint arXiv:1409.1556* (2014).
- [25] Deng, Jia, Wei Dong, Richard Socher, Li-Jia Li, Kai Li, and Li Fei-Fei. "Imagenet: A large-scale hierarchical image database." *2009 IEEE conference on computer vision and pattern recognition*, pp. 248-255. Ieee, 2009.
- [26] Lee, Jong-Sen. "Digital image smoothing and the sigma filter." *Computer vision, graphics, and image processing* 24, no. 2 (1983): 255-269.
- [27] Wong, H. S., M. K. Head, and N. R. Buenfeld. "Pore segmentation of cement-based materials from backscattered electron images." *Cement and concrete research* 36, no. 6 (2006): 1083-1090.
- [28] Constantinides, Georgios, and Franz-Josef Ulm. "The effect of two types of CSH on the elasticity of cement-based materials: Results from nanoindentation and micromechanical modeling." *Cement and concrete research* 34, no. 1 (2004): 67-80.
- [29] Nguyen, Dan-Tam, Rouhollah Alizadeh, James J. Beaudoin, Pouya Pourbeik, and Laila Raki. "Microindentation creep of monophasic calcium–silicate–hydrates." *Cement and Concrete Composites* 48 (2014): 118-126.